

THE OFFICIAL MAGAZINE OF THE OCEANOGRAPHY SOCIETY

Oceanography

CITATION

Talley, L.D. 2013. Closure of the global overturning circulation through the Indian, Pacific, and Southern Oceans: Schematics and transports. *Oceanography* 26(1):80–97, <http://dx.doi.org/10.5670/oceanog.2013.07>.

DOI

<http://dx.doi.org/10.5670/oceanog.2013.07>

COPYRIGHT

This article has been published in *Oceanography*, Volume 26, Number 1, a quarterly journal of The Oceanography Society. Copyright 2013 by The Oceanography Society. All rights reserved.

USAGE

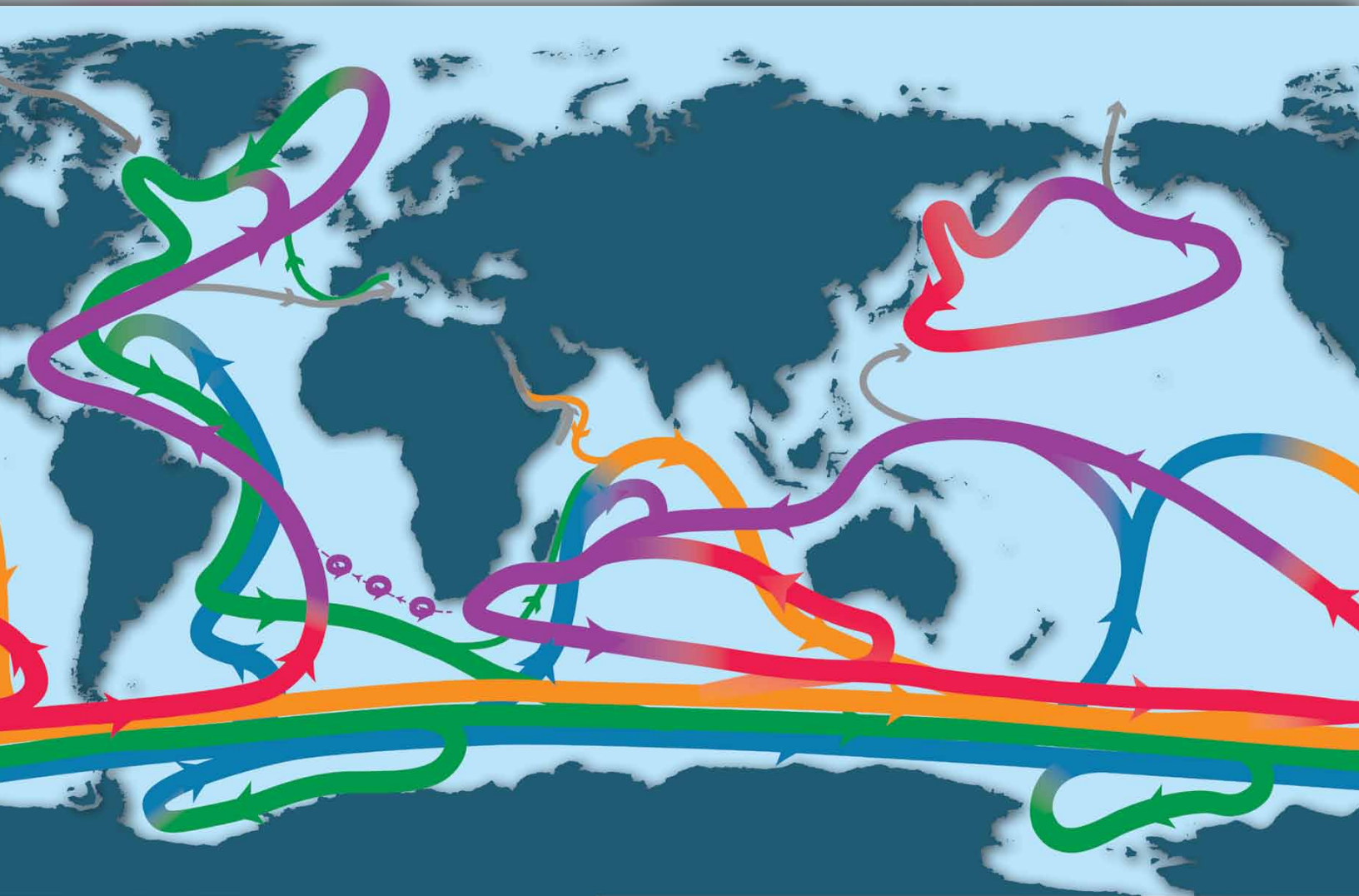
Permission is granted to copy this article for use in teaching and research. Republication, systematic reproduction, or collective redistribution of any portion of this article by photocopy machine, reposting, or other means is permitted only with the approval of The Oceanography Society. Send all correspondence to: info@tos.org or The Oceanography Society, PO Box 1931, Rockville, MD 20849-1931, USA.

SPECIAL ISSUE ON UPPER OCEAN PROCESSES:
PETER NIILER'S CONTRIBUTIONS AND INSPIRATIONS

Closure of the Global Overturning Circulation Through the Indian, Pacific, and Southern Oceans

Schematics and Transports

BY LYNNE D. TALLEY



ABSTRACT. The overturning pathways for the surface-ventilated North Atlantic Deep Water (NADW) and Antarctic Bottom Water (AABW) and the diffusively formed Indian Deep Water (IDW) and Pacific Deep Water (PDW) are intertwined. The global overturning circulation (GOC) includes both large wind-driven upwelling in the Southern Ocean and important internal diapycnal transformation in the deep Indian and Pacific Oceans. All three northern-source Deep Waters (NADW, IDW, PDW) move southward and upwell in the Southern Ocean. AABW is produced from the denser, salty NADW and a portion of the lighter, low oxygen IDW/PDW that upwells above and north of NADW. The remaining upwelled IDW/PDW stays near the surface, moving into the subtropical thermoclines, and ultimately sources about one-third of the NADW. Another third of the NADW comes from AABW upwelling in the Atlantic. The remaining third comes from AABW upwelling to the thermocline in the Indian-Pacific. Atlantic cooling associated with NADW formation (0.3 PW north of 32°S; 1 PW = 10^{15} W) and Southern Ocean cooling associated with AABW formation (0.4 PW south of 32°S) are balanced mostly by 0.6 PW of deep diffusive heating in the Indian and Pacific Oceans; only 0.1 PW is gained at the surface in the Southern Ocean. Thus, while an adiabatic model of NADW global overturning driven by winds in the Southern Ocean, with buoyancy added only at the surface in the Southern Ocean, is a useful dynamical idealization, the associated heat changes require full participation of the diffusive Indian and Pacific Oceans, with a basin-averaged diffusivity on the order of the Munk value of $10^{-4} \text{ m}^2 \text{ s}^{-1}$.

INTRODUCTION

Description of the pathways and energetics of the global overturning circulation (GOC) is central to understanding the interaction of different ocean basins and layers as well as the interplay of external forcings. Changes in the ocean's overturn on decadal to millennial time scales are central to variations in Earth's climate. For many decades, the dominant paradigm of the global overturning circulation described two nearly independent cells: the popularized North Atlantic Deep Water (NADW) "great ocean conveyor," with the formation of NADW in

the northern North Atlantic returned by upwelling in the Indian and Pacific Oceans (Gordon, 1986a; Broecker, 1987), and a second cell associated with Antarctic Bottom Water (AABW) formation in the south (Gordon, 1986b, 1991; Broecker, 1991; Schmitz, 1995). Connection of the two through upwelling of AABW into NADW in the North Atlantic has long been an accepted part of the global volume transport budget.

Modern authors connect the two dominant overturning cells (e.g. Schmitz, 1995; Rahmstorf, 2002; Lumpkin and Speer, 2007; Kuhlbrodt et al., 2007).

Recent interest has been focused on the importance of wind-driven upwelling of NADW to the sea surface in the Southern Ocean, suggesting northward return flow directly out of the Southern Ocean (Toggweiler and Samuels, 1995; Gnanadesikan, 1999; Marshall and Speer, 2012). In simplest form, with no diapycnal mixing in the ocean interior, recent GOC models importantly produce this southward flow of deep waters to the Southern Ocean where they upwell to the sea surface, driven by Southern Ocean wind stress curl and the geometry of the open Drake Passage latitude band (e.g., Marshall and Radko, 2003; Wolfe and Cessi, 2011).

Tied to this is the well-known and important dynamical similarity of all three oceans—each transports deep water southward to where it rises to the surface in the Southern Ocean, and each transports bottom water northward, regardless of a northern source of deep water. The principal interocean difference is that the Atlantic deep layer is mostly sourced from the sea surface and is thus marked by tracers indicating young age (high oxygen, low nutrients), while the Pacific and Indian deep layers are almost entirely sourced from upwelled bottom waters, and hence

Lynne D. Talley (ltalley@ucsd.edu) is Professor, Scripps Institution of Oceanography, University of California, San Diego, La Jolla, CA, USA.

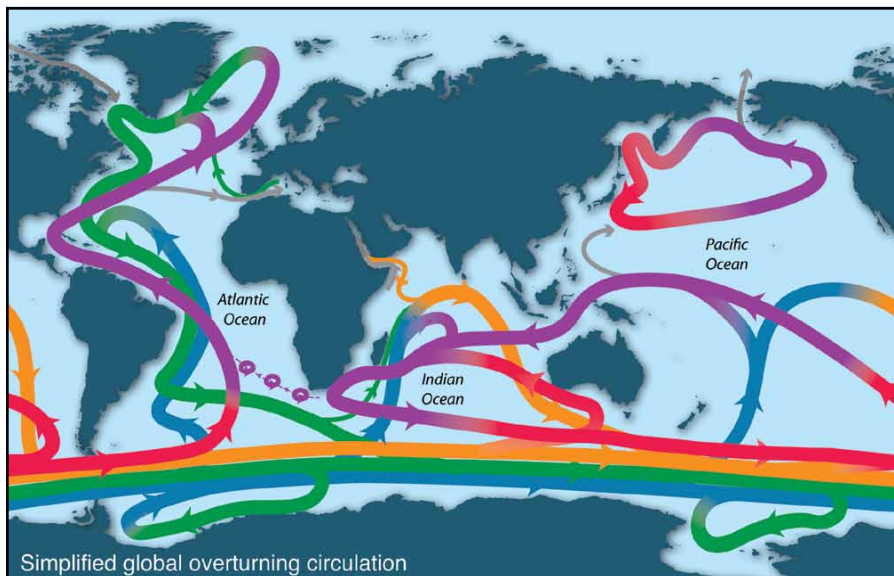


Figure 1. Schematic of the global overturning circulation. Purple = upper ocean and thermocline. Red = denser thermocline and intermediate water. Orange = Indian Deep Water and Pacific Deep Water. Green = North Atlantic Deep Water. Blue = Antarctic Bottom Water. Gray = Bering Strait components and Mediterranean and Red Sea inflows. Updated from Talley et al. (2011), based on Schmitz (1995), Rahmstorf (2002), and Lumpkin and Speer (2007).

are marked by tracers indicating much greater age (low oxygen, high nutrients).

Because of recent focus on the pivotal role of wind-driven upwelling in the Southern Ocean, the essential role of diapycnal upwelling of deep waters in the Indian and Pacific Oceans has been sidelined, but the overturning transports involved are significant (e.g., Toole and Warren, 1993; Schmitz, 1995; Robbins and Toole, 1997; Ganachaud and Wunsch, 2000, 2003; Sloyan and Rintoul, 2001; Talley et al., 2003; Lumpkin and Speer, 2007; Talley, 2008; McDonagh et al., 2008; Macdonald et al., 2009). The Indian/Pacific upwelling of AABW into the Indian and Pacific Deep Waters (IDW and PDW) is an integral step in global overturning circulation (Gordon, 1986a,b, 1991; Schmitz, 1995, 1996; Speer et al., 2000; Lumpkin and Speer, 2007; Talley, 2008), requiring diapycnal (dianeutral) diffusion in the deep Indian and Pacific Oceans, far from the

sea surface. Without diapycnal upwelling at low latitudes that forms IDW and PDW from AABW and NADW, neither AABW nor NADW could be returned eventually to their sea surface sources, particularly in terms of observed heat content. Air-sea heat gain in the Southern Ocean, invoked in Lumpkin and Speer (2007) and Marshall and Speer (2012), while important for return of upwelled deep waters to the subtropical thermocline, is only part of the required heating that must begin with warming of bottom waters, based on heat budgets shown later (see Quantifying Transports and Fluxes section), and consistent with the best estimates of Southern Ocean air-sea heat flux (Large and Yeager, 2009; Cerovečki et al., 2011).

The diapycnal diffusivities that are diagnosed from basin-scale transport budgets are not negligible (Talley et al., 2003; Lumpkin and Speer, 2007; Macdonald et al., 2009) and are

consistent with independent and direct estimates of deepwater diffusivities, averaging $10^{-4} \text{ m}^2 \text{ s}^{-1}$ (recent work of Amy Waterhouse, Scripps Institution of Oceanography, and colleagues), which is the canonical Munk (1966) value. Thus, while physical return of the deep waters to the sea surface is almost certainly dynamically controlled by Southern Ocean winds, the properties and especially heat content of the upwelled waters depend strongly on diffusion at low latitudes and the pathway of abyssal and deep waters through the Indian and Pacific Oceans.

Schematics of the GOC presented in two later sections of this paper illustrate the intertwined NADW, AABW, IDW, and PDW cells, as well as the dominant location of northward upper ocean transports out of the Southern Ocean. They are revisions of schematics published as part of a textbook explanation of the GOC (Talley et al., 2011) and owe a great deal to previous work, particularly Gordon (1991), Schmitz (1995, 1996), and Lumpkin and Speer (2007). The GOC pathways in the global map of Figure 1, based on Talley et al. (2011), are similar to those of Marshall and Speer (2012), illustrating convergence in thinking about the GOC. The pathways are associated in the Quantifying Transports and Fluxes section with quantitative transports and energy balances from Talley (2008).

The most important aspect emphasized here is the role in the NADW and AABW energy balance of the volumetrically large upwelling in the Indian and Pacific Oceans from abyssal to deep waters. The deep, diapycnal warming in the Indian and Pacific accomplishes most of the heating needed to return

NADW and AABW to the upper ocean (see Quantifying Transports and Fluxes section). It is also important to stress that the IDW and PDW, which are lighter than the NADW, upwell to the sea surface in the Southern Ocean *above* and *north* of the upwelled NADW (see next section). The upwelled IDW/PDW is thus hypothesized to be the dominant source of the upper ocean waters that leave the Southern Ocean (Subantarctic Mode Water or SAMW), flow through the subtropical thermoclines of the Indian and Pacific Oceans, and eventually make their way to the northern North Atlantic to feed the NADW (Speer et al., 2000; Lumpkin and Speer, 2007; Talley, 2008). The enhanced nutrient content of SAMW is evidence of its origin as upwelled IDW/PDW, and is essential to the biological productivity of much of the world ocean's thermocline (Sarmiento et al., 2004).

RELATIONSHIP BETWEEN NADW, IDW, AND PDW IN THE SOUTHERN HEMISPHERE

North Atlantic Deep Water upwells to the upper ocean in the Southern Ocean, where it becomes a source of Antarctic Bottom Water. Warren (1990) reiterates¹ this classic concept, which was based on water mass properties (Merz and Wüst, 1922), and moreover identifies the NADW core isopycnal as that which matches the sill depth of the Drake Passage latitude band (with the shallowest region actually being south of New Zealand). Meridional geostrophic flow on isopycnals that are denser than

this can cross the open latitude band of Drake Passage (roughly 57° to 61°S, sill depth of about 2,000 m), while water on shallower isopycnals must connect through some process other than net meridional geostrophic transport (Gill and Bryan, 1971; Toggweiler and Samuels, 1995). Another way of stating this special circumstance is that shallow isopycnals that outcrop in the Drake Passage latitude band are continuous all the way around Antarctica and cannot support net east-west pressure gradients, which means that they cannot support net meridional geostrophic flow. Isopycnals that are deep enough can intersect the ocean bottom at a ridge, which can act as a deep meridional boundary, and therefore support a zonal pressure gradient and net meridional geostrophic flow. The same, of course, is true of any surface isopycnal outcrop that intersects a coastline either north or south of Drake Passage (any of the

continents to the north, or Antarctica to the south), and can therefore support meridional geostrophic flow.

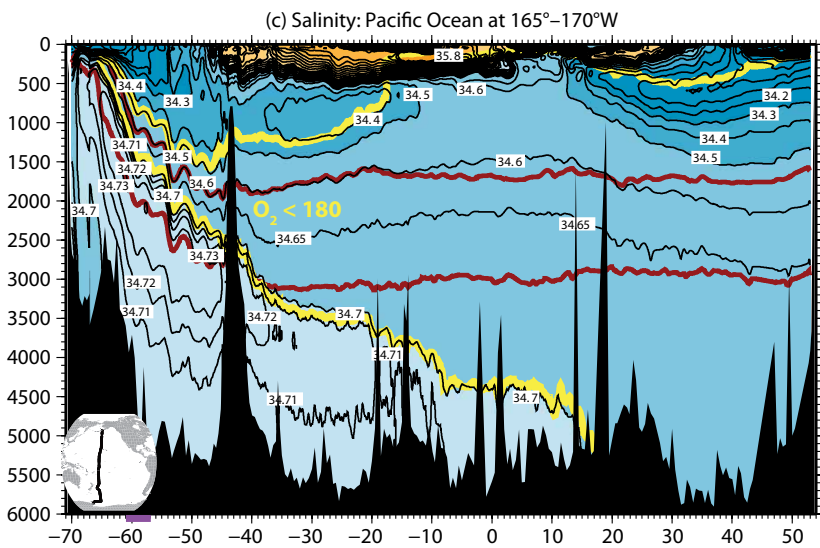
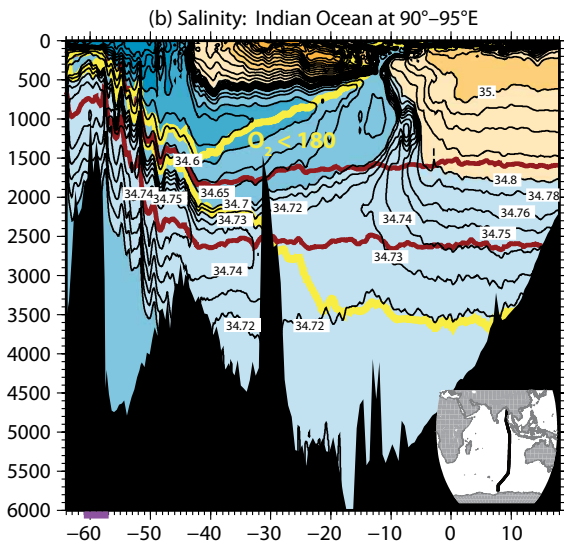
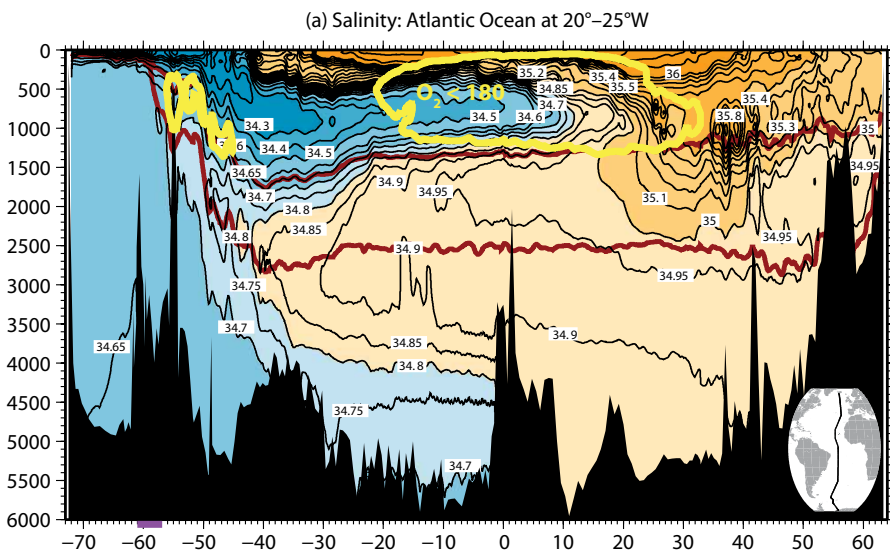
This rise of NADW across the Antarctic Circumpolar Current (ACC) is marked by high salinity in all three oceans, from about 3,000 m depth up to about 400 m depth in the Pacific sector, to 800 m in the Indian, and within the upper 200 m in the Weddell Sea (Atlantic sector) (Figure 2). The isoneutral surface $\gamma^N = 28.04 \text{ kg m}^{-3}$ (Jackett and McDougall, 1997) tracks the salinity maximum of the NADW in the ACC in all oceans (heavy dark red in Figure 2). This is approximately the same as the potential density surface $\sigma_\theta = 27.8 \text{ kg m}^{-3}$ that Warren (1990) identified as approximately the densest isopycnal crossing Drake Passage at sill depth. Orsi and Whitworth (2004) chose $\gamma^N = 28.05 \text{ kg m}^{-3}$ for mapping this layer in their Southern Ocean atlas.

This NADW isoneutral surface

¹ "Thus, because of Drake Passage and the field of wind-stress curl, which draws the deep water of the Southern Ocean to the sea surface, Antarctic Bottom Water is just recycled North Atlantic Deep Water."

ACRONYMS

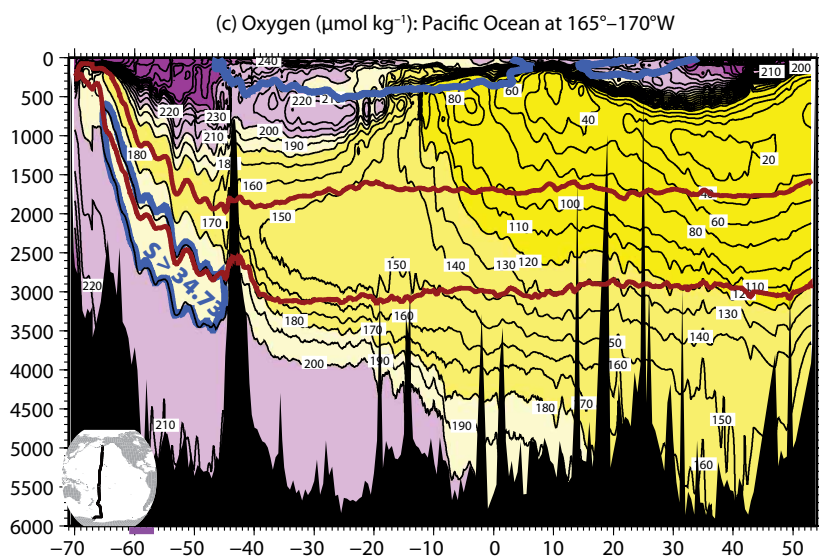
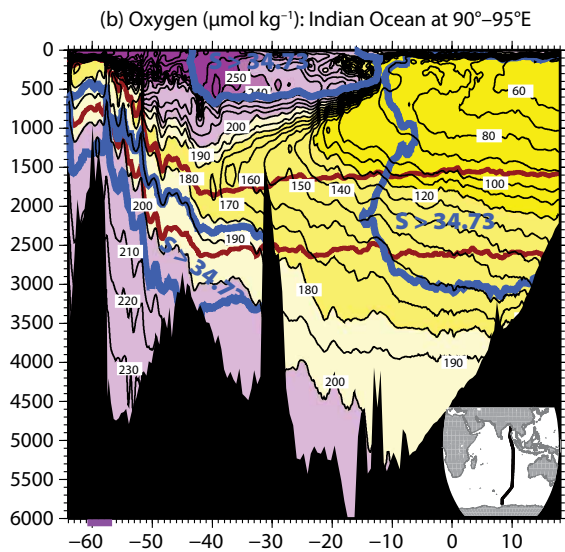
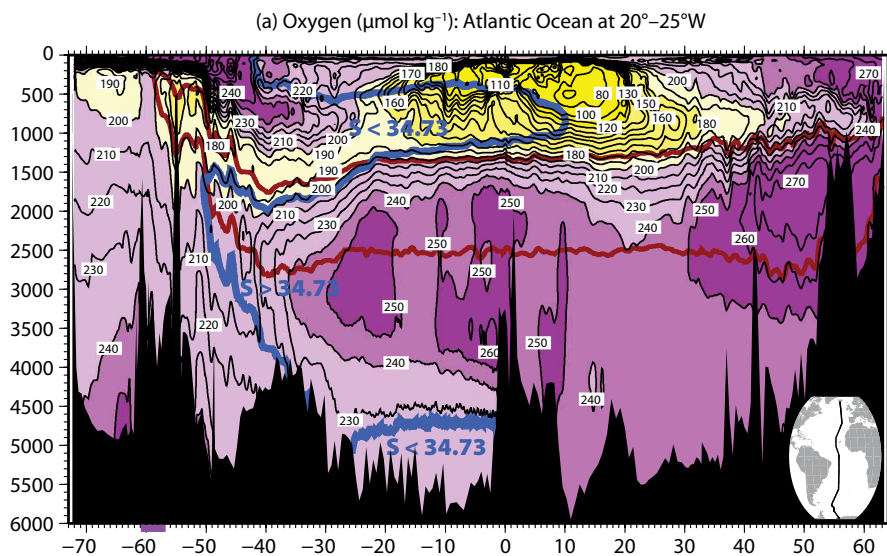
AABW.....	Antarctic Bottom Water
AAIW.....	Antarctic Intermediate Water
ACC.....	Antarctic Circumpolar Current
CDW.....	Circumpolar Deep Water
GOC.....	Global Overturning Circulation
IDW.....	Indian Deep Water
LCDW.....	Lower Circumpolar Deep Water
NADW.....	North Atlantic Deep Water
NPIW.....	North Pacific Intermediate Water
PDW.....	Pacific Deep Water
SAF.....	Subantarctic Front
SAMW.....	Subantarctic Mode Water
UCDW.....	Upper Circumpolar Deep Water



reaches the sea surface only south of the ACC, based on salinity and oxygen sections (examples in Figures 2 and 3), and oxygen mapped on the NADW isoneutral surface (Orsi and Whitworth, 2004). That is, it reaches the surface in the Weddell Sea and western Ross Sea where new water is being produced at this density, and otherwise only very close to the Antarctic coast where it lies beneath weak or easterly winds. Within the ACC, the NADW lies beneath the IDW and PDW, described next.

Indian and Pacific Deep Waters also upwell to the sea surface in the Southern Ocean. Their core is identified by low oxygen (Figure 3). They are less dense and lie above the NADW. The core isoneutral surface marking this low oxygen IDW/PDW is $\gamma^N = 27.8 \text{ kg m}^{-3}$. Orsi and Whitworth (2004) chose $\gamma^N = 27.84 \text{ kg m}^{-3}$ to characterize this water mass. The IDW/PDW isoneutral surface outcrops within the ACC, mostly south of the Polar Front. Therefore, the surface waters originating as outcropped IDW/PDW are accessible to

Figure 2. Salinity for the (a) Atlantic (20°–25°W), (b) Indian (80°–95°E), and (c) Pacific (165°–170°W) Oceans. The $180 \mu\text{mol kg}^{-1}$ oxygen contour (heavy yellow) illustrates the oxygen minimum in the Southern Ocean, which originates in the Indian and Pacific Oceans (Indian Deep Water and Pacific Deep Water) and lies above the salinity maximum that originates in the North Atlantic (North Atlantic Deep Water). Isoneutral contours $\gamma^N = 27.8$ and 28.04 kg m^{-3} (heavy dark red) represent the cores of the low oxygen Indian Deep Water/Pacific Deep Water and high-salinity North Atlantic Deep Water components, respectively. Section locations are indicated on inset maps. The heavy purple line segment on the latitude axes marks the Drake Passage latitude band (61°–57°S). For further information on these sections, including other measured properties and data sets, see the World Ocean Circulation Experiment atlases (Orsi and Whitworth, 2004; Talley, 2007, 2011; Koltermann et al., 2011).



the northward Ekman transport driven by the Westerlies across the Polar and Subantarctic Fronts (the latter being the northernmost front of the ACC).

From transport budgets presented later in the Quantifying Transports and Fluxes section, which yield a total of 29 Sv formation of Antarctic Bottom Water (1 Sv = 1 Sverdrup = $1 \times 10^6 \text{ m}^3 \text{ s}^{-1}$), consistent with various independent formation rate estimates based on different methods (see Talley, 2008), not only is it clear that all of the southward (13 of the total 18 Sv) NADW transport is required to feed AABW, but also a substantial fraction of the IDW/PDW. Because of the very clear layering of the IDW/PDW oxygen minimum above the NADW salinity maximum at every longitude along the ACC, and because the IDW/PDW surface outcrop lies well within the ACC, upwelled IDW/PDW is the most likely source water for the northward flow across the Subantarctic Front into the thick surface layer of the Subantarctic Mode Water. The elevated nutrients delivered by the

Figure 3. Oxygen ($\mu\text{mol kg}^{-1}$) for the (a) Atlantic (20° – 25°W), (b) Indian (80° – 95°E), and (c) Pacific (165° – 170°W) Oceans. The 34.73 salinity contour (heavy blue) illustrates the salinity maximum in the Southern Ocean, which originates in the North Atlantic (North Atlantic Deep Water) and lies beneath the oxygen minimum that originates in the Indian and Pacific Oceans (Indian and Pacific Deep Waters). The accompanying salinity sections are shown in Figure 2. Isonneutral contours $\gamma^N = 27.8$ and 28.04 kg m^{-3} (heavy dark red) represent the cores of the low oxygen Indian Deep Water/Pacific Deep Water and high-salinity North Atlantic Deep Water components, respectively. Section locations are indicated on inset maps. The heavy purple line segment on the latitude axes marks the Drake Passage latitude band (61° – 57°S). For further information on these sections, including other measured properties and data sets, see the World Ocean Circulation Experiment atlases (Orsi and Whitworth, 2004; Talley, 2007, 2011; Koltermann et al., 2011).

SAMW to the thermocline are evidence of the upwelled nutrient-rich IDW/PDW component (Sarmiento et al., 2004).

The implication of the above is that NADW entering the ACC does not return directly to the sea surface to be blown northward to the Atlantic thermocline. The route for return of NADW to the sea surface thus passes through (1) AABW formation, (2) northward flow into the deep oceans to the north, (3) upwelling into the IDW/PDW layer, which returns to the Southern Ocean, (4) upwelling of IDW/PDW to the sea surface, and (5) northward surface flow

(of a portion of the upwelled water) into the thermoclines and hence the return flow to the North Atlantic.

This assumption of the pathways for NADW, IDW, and PDW is strongly supported by the heat/energy budget presented later in the section on Quantifying Transports and Fluxes. There is not enough surface heating in the Southern Ocean to return NADW to the thermocline (nor is there enough Southern Ocean heating to return the AABW back to its sea surface sources.) However, a significant amount of heating reaches the deep Indian and Pacific

Oceans; it elevates AABW to IDW/PDW, which is less dense than NADW. The warming that does occur at the sea surface in the Southern Ocean then accounts for the further elevation of a portion of the IDW/PDW to the SAMW and the base of the subtropical thermocline.

THREE-DIMENSIONAL SCHEMATICS OF THE GLOBAL OVERTURNING CIRCULATION

Schematics of the circulation that include the overturning and upwelling branches that account for the large interbasin transports and heat redistribution necessarily oversimplify the time-dependent and partially turbulent movement of water through the ocean, but they are useful for framing the ongoing discussion of the dynamics and pathways of the actual overturning circulation. Richardson (2008) summarizes overturning schematics dating back to the nineteenth century, showing the evolving understanding of the Atlantic and global overturning.

The revised schematics of the global overturning circulation presented here (Figures 1 and 4, and later Figure 5) are updated from Talley et al. (2011). They (1) refine the global mapping view, similar to recent maps published by Schmitz (1995), Lumpkin and Speer (2007), Kuhlbrodt et al. (2007), Talley (2008), and Marshall and Speer (2012) (Figure 1); (2) refine the Southern Ocean-centric schematic introduced by Gordon (1991) that was subsequently revised by Schmitz (1996) and then again by Lumpkin and Speer (2007) (Figure 4); and (3) introduce a new two-dimensional representation of the global overturning streamfunction (see Figure 5

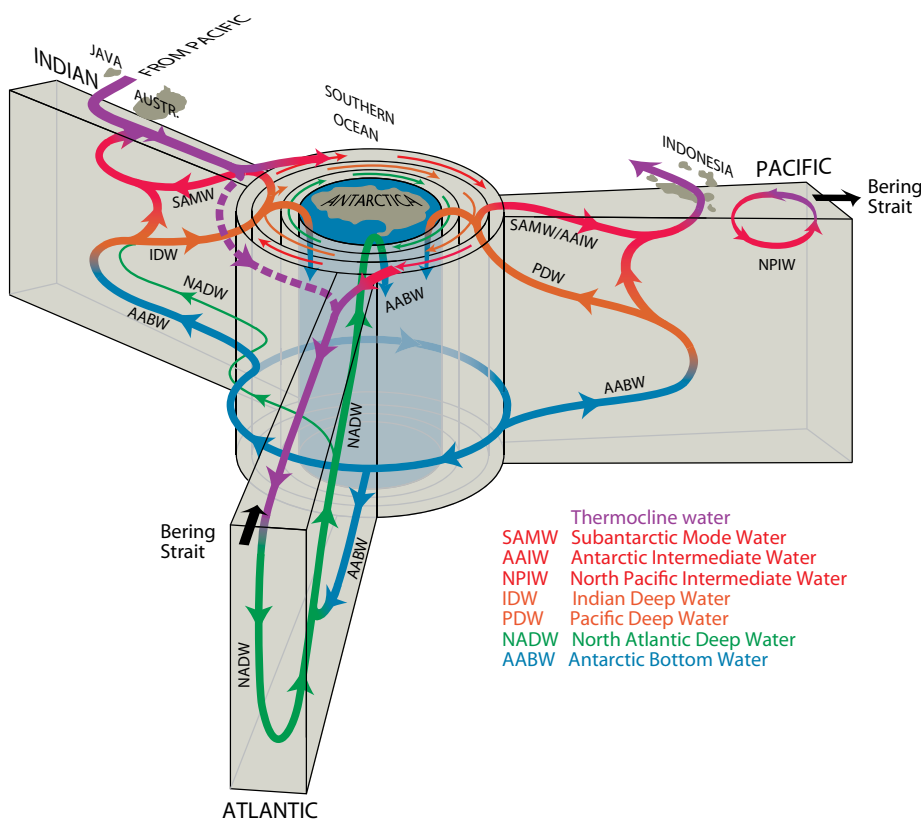


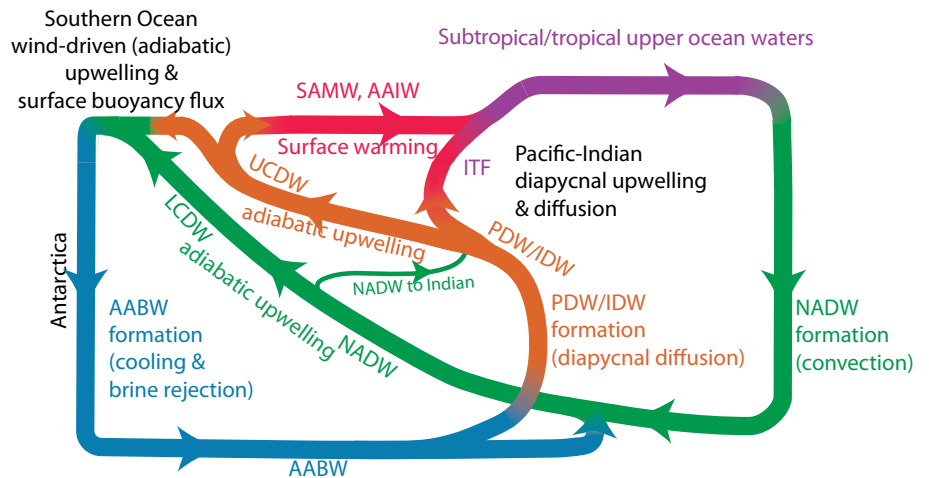
Figure 4. Schematic of the overturning circulation from a Southern Ocean perspective, revised from Talley et al. (2011), after Gordon (1986), Schmitz (1995), and Lumpkin and Speer (2007). Southern Ocean outcropping of the high-salinity NADW is depicted far to the south, with conversion into AABW close to Antarctica (blue cylinder, with formation at many locations). The low oxygen Pacific and Indian Deep Water (PDW/IDW) layers, which outcrop farther north in the Antarctic Circumpolar Current, are the most direct source of the surface water that flows northward out of the Southern Ocean and into the subtropical thermoclines (SAMW/AAIW). The self-contained and weak NPIW overturn is also indicated in the North Pacific.

and later discussion).

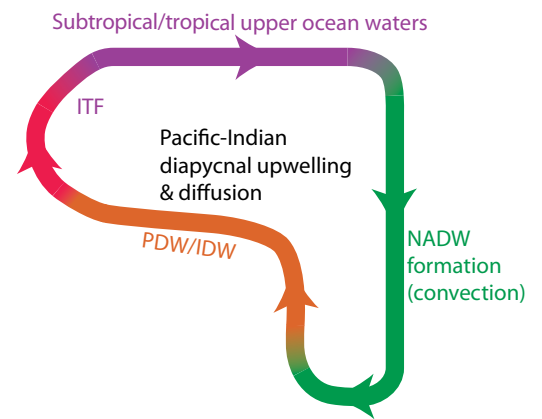
Quantitative transports that are the basis of these schematics are described in Quantifying Transports and Fluxes below, and are consistent with other quantitative analyses of the GOC. The separate roles of the IDW/PDW and NADW are described above, and are the basis for the hypothesis at the heart of these schematics, that the IDW/PDW outcrops north of the NADW in the Southern Ocean, and a portion of its transport is the dominant source of the northward flow of surface waters into the Southern Hemisphere thermocline, rather than the NADW.

Like all schematics, this set has its particular oversimplifications. Perhaps most importantly, the shallow overturning cells in the tropics and subtropics are omitted; they transport much of the poleward heat out of the tropics and redistribute much of the freshwater (e.g., Talley, 2003, 2008). A second oversimplification is that no schematic adequately represents the mixing that blurs the distinctions between juxtaposed water masses as they move along together and in fact circulate in the same

(a) Southern Ocean and low latitude Indian/Pacific upwelling



(b) Low latitude Indian/Pacific upwelling (missing Southern Ocean)



(c) Southern Ocean upwelling (missing low latitude upwelling)

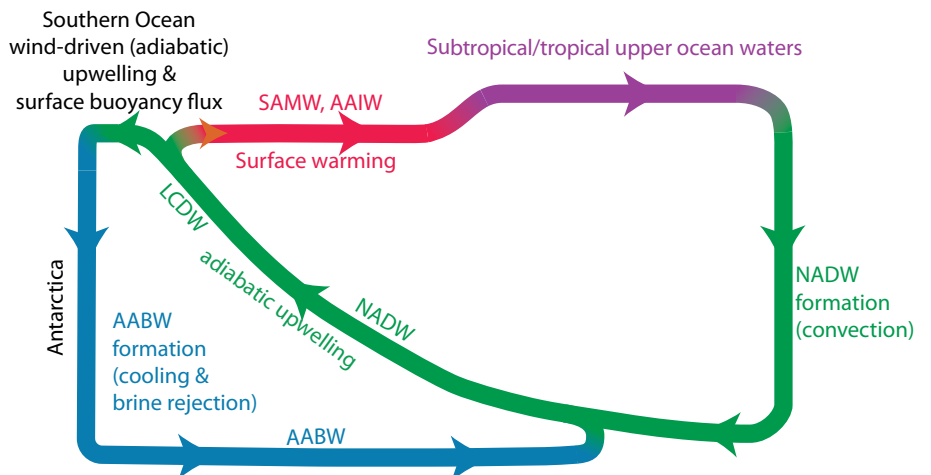


Figure 5. Schematic of the overturning circulation in a two-dimensional view, with important physical processes listed, revised from Talley et al. (2011). Colors as in Figures 1 and 4. (a) Most complete version, including North Atlantic Deep Water (NADW) and Antarctic Bottom Water (AABW) cells, and upwelling in the Southern, Indian, and Pacific Oceans. (b) Incomplete single cell schematic, corresponding to the Gordon (1986a,b) and Broecker (1991) "conveyor belt," which (intentionally) was associated with the global NADW circulation, excluding AABW, but thereby incorrectly excluded Southern Ocean upwelling of NADW. (c) Incomplete two-cell schematic, emphasizing the NADW and AABW cells, closely resembling the globally zonally averaged streamfunction.

isopycnal layers. An especially clear example is the penetration of Southern Ocean deep waters (Circumpolar Deep Water) far to the north in the Atlantic Ocean, including within isoneutral layers dominated in transport by the southward flow of NADW (e.g. Reid, 1994).

The GOC schematics include four layers—upper ocean/thermocline, intermediate, deep, and bottom—as in Schmitz (1995). The two major global cells are (1) the North Atlantic Deep Water cell, with dense water formation at sites around the northern North Atlantic² and (2) the Antarctic Bottom Water cell, with dense water formation around Antarctica. These two cells are interconnected, especially in the Southern Ocean, complicating any simple representation of the overturn. A third, weak, overturning cell is found in the North Pacific, forming a small amount (order 2 Sv) of intermediate water (North Pacific Intermediate Water or NPIW). It is mostly unconnected to the NADW/AABW cells, but is important to note because it is the North Pacific's very weak analog of NADW formation; the strong vertical stratification in the North Pacific disallows deepwater formation.

The two other major deep waters of the world ocean represented here, Pacific Deep Water and Indian Deep Water, are formed diffusively within their respective oceans from inflowing NADW and AABW, and not from surface sources within these basins. These waters are therefore “old,” marked by low oxygen and high nutrient content.³ (A fifth

major deep water mass is Circumpolar Deep Water [CDW], formed in the Southern Ocean; CDW includes NADW, IDW, and PDW, and also locally forms dense waters, such as Weddell and Ross Deep Waters, that are not quite dense enough to become AABW. CDW is transported northward out of the Southern Ocean into the same isopycnal ranges as the southward-flowing northern deep waters, but the net transport in these layers is dominated by the NADW, IDW, and PDW.)

Global NADW Cell

We start the NADW cell description with its upper ocean and thermocline sources, which enter the Atlantic from the Pacific (via Drake Passage) and Indian Oceans (via the Agulhas).

The upper ocean source water from the Drake Passage region includes Antarctic Intermediate Water (AAIW) and surface waters from just north of the Antarctic Circumpolar Current, including Subantarctic Mode Water. SAMW and AAIW include a substantial contribution from northward (Ekman) transport of surface waters across the ACC that arises from upwelling of IDW and PDW in the northern part of the ACC.

The upper ocean source water from the Agulhas is composed of: (1) upwelled deep waters from within the Indian Ocean, (2) upwelled deep waters from the Pacific Ocean, (3) subducted upper ocean waters from the southeastern Indian Ocean, and (4) subducted upper ocean waters from the southeastern

Pacific. The Pacific waters [(2) and (4), above] mostly enter the Indian Ocean through the Indonesian Throughflow (ITF), with additional “leakage” south of Australia (Speich et al., 2002; Lumpkin and Speer, 2007). The subducted waters [(3) and (4) above] include ACC surface waters that join the Subantarctic Mode Water, as described in the previous paragraph. The Agulhas and Drake Passage pathways are connected. Most of the Agulhas waters turn southeastward rather than entering the Atlantic, losing heat on the southeastward path along the Agulhas Return Current, before joining the SAMW and ultimately entering the Atlantic as cooler SAMW and AAIW rather than warm Agulhas waters.

Figures 1 and 4 depict the small leakage of less than 1 Sv from the Pacific through Bering Strait to the Arctic and onward to the dense water formation sites in the Labrador and Nordic Seas. It becomes part of the NADW that flows southward through the Atlantic. It is not possible to ascribe its source in the Pacific to any one particular layer or location, but it does represent a freshwater and volume flux from the Pacific to the Atlantic. (Talley [2008] details the implications of this flow for the properties of both NADW and NPIW, showing that the Bering Strait leakage is but a minor contributor to the NADW freshening relative to its subtropical Atlantic surface sources with most freshening due to net precipitation in the subpolar North Atlantic. However, the much weaker NPIW overturn is strongly

² “NADW” here includes Nordic Seas Overflow Waters, Labrador Sea Water, and Mediterranean Overflow Water. “AABW” here includes all dense waters that form around Antarctica and that advect northward into the abyssal basins; it is synonymous with Circumpolar Deep Water (CDW) in this simplified view, but in more detailed water mass analyses, “AABW” refers just to the densest CDW. See Chapters 9 and 13 in Talley et al. (2011) for detailed definitions of Atlantic and Southern Ocean water masses.

³ A small trickle of Red Sea Water adds high salinity to the deep northern Indian Ocean but does not measurably affect its ventilation age because it can entrain only the ambient old waters, unlike the similarly small-volume sources in the North Atlantic that entrain newly ventilated waters.

controlled by the Bering Strait freshwater export from the Pacific.)

In the Atlantic, the joined Agulhas and Drake Passage upper ocean water moves northward through the complex surface gyre systems, cooling and finally sinking at the several well-known dense water formation sites around the northern North Atlantic (Nordic Seas, Labrador Sea, and Mediterranean Sea). These denser (cooler and also mostly fresher) waters move southward at depth and exit the North Atlantic as NADW. Beneath the southward transport of NADW, AABW moves northward. It upwells into the bottom of the NADW layer, in a diffusively controlled process, and then returns southward as part of the NADW. The pathway of AABW in the Indian and Pacific Oceans is described in the next section.

The NADW exits the Atlantic just south of Africa and joins the eastward flow in the Southern Ocean. Some moves northward into the southwest Indian Ocean near the Agulhas where it joins the Indian's upwelling AABW to form the (slightly less dense) Indian Deep Water. However, most of the NADW enters and crosses the ACC and upwells to the sea surface in the regions south of the ACC. Here, it becomes part of the surface source for dense water formation processes around Antarctica, which produce AABW as well as the local deep waters.

Note that in the Lumpkin and Speer (2007) transport analysis, there is enough NADW of lower density ($\sigma_\theta < 27.6 \text{ kg m}^{-3}$) exiting the Atlantic to join the more northerly upwelling of IDW and PDW that feeds northward Ekman transport across the ACC, as described below. Transports of NADW at these lower densities in the present

(Reid, 1994, 1997, 2003) analysis are not significant, and so this direct pathway for return of NADW to the Southern Ocean sea surface did not emerge, similar to other earlier results showing a potential density σ_θ of around 27.6 kg m^{-3} for the top of the NADW layer in the Southern Ocean, summarized in Gordon (1986a).

In all three oceans, AABW upwells into the local deep water, that is, into the NADW, IDW, and PDW. Because there is no dense water formation in the North Pacific, this upwelled AABW is the sole source of the PDW. AABW is by far the largest contributor to IDW as well, with much less direct input from NADW and

DESCRIPTION OF THE PATHWAYS AND ENERGETICS OF THE GLOBAL OVERTURNING CIRCULATION IS CENTRAL TO UNDERSTANDING THE INTERACTION OF DIFFERENT OCEAN BASINS AND LAYERS AS WELL AS THE INTERPLAY OF EXTERNAL FORCINGS.

Global AABW Cell

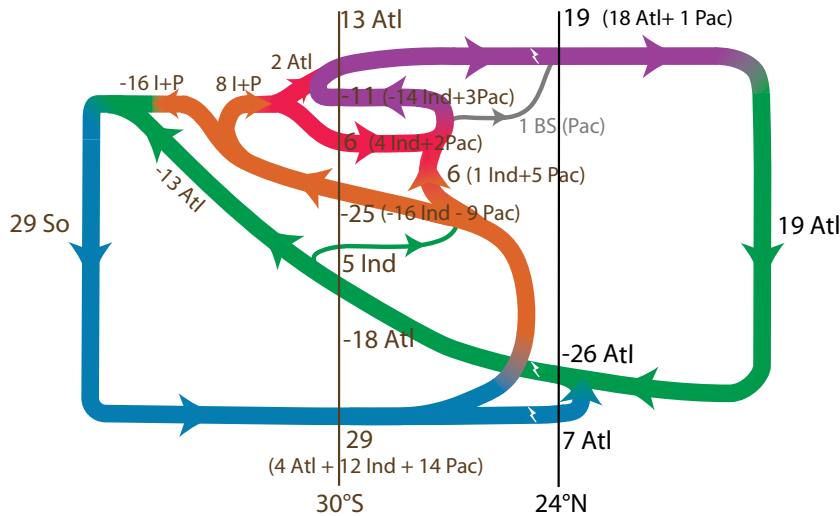
The AABW cell description begins with upwelling of the NADW in the Southern Ocean to near the sea surface around Antarctica, where it is cooled to freezing. It is freshened by net precipitation and mixing with near-surface fresher waters that result from sea ice melt, but is also subjected to brine rejection due to sea ice formation. Some of this upwelled surface water becomes dense enough to sink and becomes the deep water that manages to escape northward across topography and into the Atlantic, Indian, and Pacific Oceans. The very densest bottom waters are confined to the Southern Ocean, but much of the new deep water is not dense enough to become AABW, but rather fills much of the water column in the Weddell Sea as Weddell Deep Water and the Ross Sea as Ross Sea Deep Water. The escaping AABW moves northward at the bottoms of the Atlantic, Indian, and Pacific Oceans.

even less from Red Sea Overflow Water. On the other hand, AABW is only a minor component of NADW compared with its northern sources that arise from Atlantic surface waters.

Connection of NADW and AABW Through IDW/PDW

IDW and PDW are formed mostly from upwelled AABW within the Indian and Pacific Oceans, north of 32°S . IDW/PDW is made up of old water masses, with their low oxygen being especially useful for tracing them as they move southward into the Southern Ocean (Figure 3). Here they lie *above* the NADW layer because they are less dense than NADW, which is marked by high salinity in the Southern Ocean (Figure 2). Here, like NADW, they upwell to the sea surface but farther to the north than the denser NADW. The upwelled IDW/PDW in the Southern Ocean feeds two cells: (1) northward flux

(a) Mass transports (Sv) for the Global Overturning Circulation



(b) Heat transport convergences (PW)

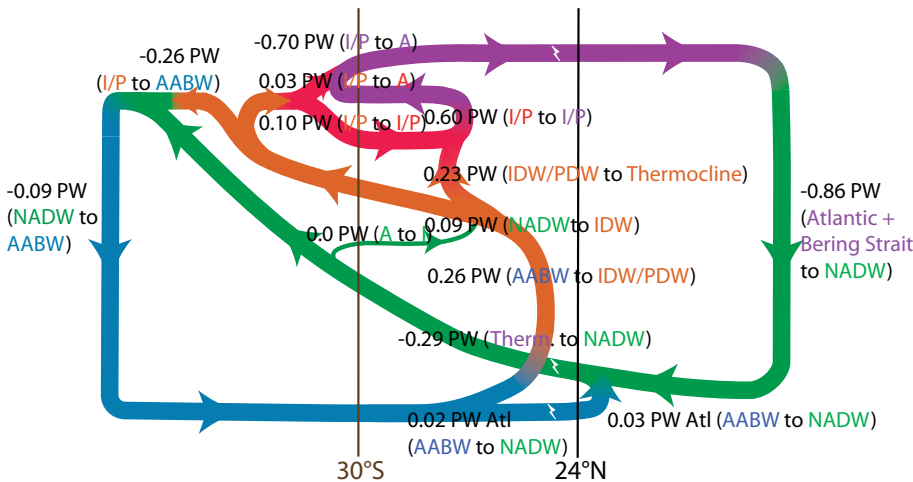


Figure 6. (a) Mass transports (in Sverdrups; 1 Sverdrup = $10^6 \text{ m}^3 \text{ s}^{-1}$) for each branch of the global overturning circulation, based on transports in isopycnal layers in Talley's (2008) Tables 9–14, and on the author's more recent work, where the assumed conversions from one water mass to another are provided. (b) Heat transport convergence (in Petawatts; 1 PW = 10^{15} W) for each mass-balanced conversion shown in (a), also based on Talley (2008) and the author's more recent work. Each number shows the net air-sea heat flux within the ocean sector that is associated with the conversion. Negative is heat loss; positive is heat gain. For instance, in the Southern Ocean, south of 30°S , the heat transport convergence of “ -0.09 PW (NADW to AABW)” means that 0.09 PW is lost from the ocean to the atmosphere south of 30°S associated with converting North Atlantic Deep Water (NADW) to Antarctic Bottom Water (AABW). Meridional heat transports associated with the upper ocean subtropical gyres are not included in (b).

of surface water across the ACC, accomplished by Ekman transport, that joins the upper ocean circulation, and (2) the dense AABW formation, which then recycles this mass back through the deep water routes, along with the NADW. The first of these is a major source of the upper ocean waters that then feed northward to the NADW formation region, again connecting the AABW and NADW cells.

TWO-DIMENSIONAL SCHEMATIC OF THE GLOBAL OVERTURNING CIRCULATION

The vertical pathways connecting NADW, AABW, IDW, and PDW are illustrated in Figure 5a, which is a flattened, two-dimensional version of Figures 1 and 4. The usual two-dimensional global schematics routinely overlook the separate nature of the NADW and IDW/PDW upwelling. This new figure repairs that omission, but in so doing is perhaps more difficult to follow than the three-dimensional schematic of Figure 4. The volume and heat transports associated with part of the GOC are detailed in the next section and are shown in Figure 6. The latter has more detail in the upper ocean layers to represent the complicated path taken by Agulhas waters and SAMW. The following describes the Figure 6 schematic.

1. Upper ocean (thermocline and above) waters (purple) move northward, ultimately reaching the North Atlantic (advection with surface-driven buoyancy transformations).
2. NADW (green) forms in the north (convection) and moves southward to the Southern Ocean (adiabatic advection). One small NADW branch exits directly to the Indian

Ocean. The remainder, identified by its high salinity core but sufficiently modified by mixing and injection of locally-formed deep waters that it is called LCDW, upwells to near the surface in the Southern Ocean (wind-driven upwelling).

3. The upwelled NADW/LCDW (green) becomes denser and sinks as AABW (blue; cooling and brine rejection). Part of the upwelled less dense IDW and PDW (orange) joins this AABW formation.
4. AABW (blue) moves northward at the bottom (adiabatic advection). It upwells in the subtropics and tropics into IDW and PDW (orange), and also into NADW (green; upwelling with diapycnal diffusion).
5. IDW and PDW (orange) return to the Southern Ocean above the NADW, forming the core of UCDW, which is identified by low oxygen (adiabatic advection). Part of it joins the NADW/UCDW to form AABW, and the rest moves northward at the sea surface as the principal source of northward flux out of the Southern Ocean. These waters are freshened and warmed and join the SAMW/AAIW (red) at the base of the subtropical thermocline (advection with surface buoyancy fluxes).
6. Upwelling of bottom and deep waters in the Indian and Pacific to the thermocline (orange to red and purple) returns part of the AABW and NADW to the sea surface (low latitude upwelling with diapycnal diffusion).
7. The joined thermocline waters (SAMW/AAIW from the Southern Ocean and upwelled thermocline water from the Indian/Pacific) become

the upper ocean transport moving toward the North Atlantic (step 1). This two-dimensional version of the GOC is similar to older but less complete scenarios of the overturning circulation. It is essentially a combination of the “Indian-Pacific upwelling” schematic for the global NADW circulation (Figure 5b) and a schematic of the global overturn based on zonally averaging over all three oceans (Figure 5c). The most important element that is added to form Figure 5a is the role of the Indian and Pacific Deep Waters in partially returning AABW to lower density, a return of these deep waters to the Southern Ocean, and completion of upwelling to the sea surface there.

The low-latitude Indian-Pacific upwelling model (Figure 5b) is the original popularized “conveyor belt” for the global NADW circulation based on Broecker (1991) and Gordon, (1986a). (Both authors also separately described the AABW global cell at about the same time but did not clarify the connection between the NADW and AABW global cells [Gordon, 1986b; Broecker, 1991; Gordon, 1991, as reproduced in Richardson, 2008].) Return of NADW to the sea surface and back to the Atlantic in this “conveyor” was hypothesized to be entirely in the mid-latitude Indian and Pacific Oceans, without the essential multiple steps of Southern Ocean upwelling.

The second incomplete scenario (Figure 5c) is a two-cell system in which AABW upwells into the bottom of NADW and the combined deep water upwells to the surface only in the Southern Ocean. If we were to sketch the NADW and AABW cells directly from accurate zonally averaged global meridional overturning streamfunctions

(e.g., Maltrud and McClean, 2005; Kuhlbrodt et al., 2007; Lumpkin and Speer, 2007), we would draw these pole-to-pole cells (Gordon, 1986b). This gives an incorrect impression that the upwelled water splits into one part flowing northward to feed NADW overturn and one part converting to AABW around Antarctica. This “Southern Ocean upwelling” scenario ignores the large-scale, large-volume upwelling in the Indian and Pacific Oceans, which ratchets the deep waters up to a density lower than NADW even though the diffusive processes are weak in comparison with direct air-sea buoyancy fluxes at the sea surface. The IDW/PDW then reenters the Southern Ocean above the NADW and upwells to the sea surface where it splits into a surface branch that feeds the northward flux of surface waters that eventually feeds NADW formation, and a dense branch, joining the upwelled NADW, to form the denser AABW.

QUANTIFYING TRANSPORTS AND FLUXES

Each branch of the overturn shown in Figures 4 and 5 has a quantitative mass transport across the latitudes analyzed (Figure 6a; a northward mass transport in an isopycnal layer balanced by a southward transport in a different isopycnal layer). Each mass-balanced overturn in these figures therefore requires diapycnal transport because water crossing the latitude in one direction, say, southward, is transformed to a different density before it crosses back at a different density. The density change is accomplished by heating/cooling and changes in salinity. Therefore, each mass-balanced overturn has an associated heat transport (Figure 6b). By

calculating the heat transport associated with those mass-balanced parts of the pathway, we determine the amount of heat that was gained or lost as the water was transformed. For example, in the North Atlantic Ocean, in this particular transport analysis based on Talley (2008), 18.8 Sv of upper ocean water are transported northward across 24°N, cooled to the north of 24°N, and return

(Atlantic and Pacific) and 32°S (Atlantic, Pacific, Indian) presented in Talley (2008) and verified in more recent research by the author. The focus here is on the partitioning of the transports among the intertwined circulations through all of the ocean basins and on the heat transports required for each of these transports. This emphasis differs somewhat from Talley (2008), although

profiles, corrected to balance externally imposed net transports (Bering Strait transport of 1 Sv; Indonesian Throughflow transport of 10 Sv; annual mean Ekman transport orthogonal to each section). An uncertainty analysis was presented in Talley (2008). Heat transports are calculated using the observed temperature associated with each velocity estimate, as detailed in Talley (2003, 2008).

“ CHANGES IN THE OCEAN'S OVERTURN ON DECADAL TO MILLENNIAL TIME SCALES ARE CENTRAL TO VARIATIONS IN EARTH'S CLIMATE. ”

southward at higher density and lower temperature (Figure 6a). Calculating the heat transport across 24°N due to this mass-balanced overturn yields the associated heat loss to the north.

The process of heating or cooling (air-sea fluxes or internal diapycnal diffusion) is, of course, not determined directly from this calculation, but if the conversion must occur entirely within the ocean, below the sea surface, based on the isopycnal layers involved, then we infer that diapycnal diffusion must be the mechanism. Because air-sea fluxes are far more effective than interior ocean turbulence in changing heat and buoyancy, we assume that air-sea fluxes dominate transformations that include a pathway through the surface layers, although they could, of course, also include some diapycnal flux.

The GOC transport analysis here (Figure 6) is based on meridional transports in isopycnal layers at 24°N

the Southern Ocean partitioning based on 32°S is essentially the same. This permits us to estimate the amount of diapycnal heating due to deep diapycnal diffusion versus near-surface fluxes that can originate from surface forcing, required for returning NADW back to the sea surface in the northern North Atlantic/Nordic Seas, and also for returning IDW/PDW back to the sea surface in the Southern Ocean.

Talley (2008) and more recent work of the author detail the method for calculating transports. Briefly, absolute geostrophic velocity profiles and Ekman transports are required for the overturning transport calculation. Units for heat transport are Petawatts (PW; 1 PW = 10^{15} W). J.L. Reid provided the reference geostrophic velocity at the ocean bottom for each station pair from his publications (Reid, 1994, 1997, 2003); each geostrophic velocity profile was then calculated from the adjacent density

Mass Transports in the AABW and NADW Overturning Circulations

Here, we focus on diagnosing the overturns and connections between different layers south and north of 32°S. To the south of 32°S in Figure 6a:

1. The 18 Sv of NADW that flow across 32°S split into 5 Sv that directly enter the southwestern Indian Ocean, and 13 Sv that move southward and upwell adiabatically in the Southern Ocean. These 13 Sv are converted to AABW through cooling and brine rejection.
2. The remaining 16 Sv of the 29 Sv of AABW come from the 24 Sv of southward-moving IDW/PDW that upwell adiabatically above the NADW.
3. The other 8 Sv of the adiabatically upwelled IDW/PDW are lightened at the sea surface (freshening and warming) and feed the upper ocean SAMW and AAIW that move northward into the subtropical thermoclines of the three oceans: 6 Sv into the Indian and Pacific and 2 Sv into the Atlantic. (Note that these rates are lower than the formation rates of these water masses because of recycling within the subtropical gyres south of 32°S [Cerovečki et al., in press].)

Looking at the conversions on the north side of 32°S, the diagnosed upwellings

are all diapycnal, requiring downward diffusion of buoyancy, mostly as heat:

1. The small amount (4 to 7 Sv) of AABW that flows into the Atlantic upwells diapycnally into the bottom of the NADW, where it returns to the ACC.
2. Most (25 Sv) of the AABW flows into the Indian and Pacific, joined by the 5 Sv of NADW that entered the Indian Ocean directly from the Atlantic.
3. This joined 30 Sv quantity upwells diapycnally in the Indian/Pacific. Most (25 Sv) becomes IDW and PDW and returns to the Southern Ocean. A 6 Sv amount of the combined IDW/PDW/NADW upwells to the thermocline, mostly in the Pacific where it feeds 1 Sv northward to Bering Strait and the rest to the Indonesian Throughflow that connects to the Indian Ocean thermocline.

There is a complicated but important situation in the thermocline waters across 32°S, depicted by the zigzags of red and purple in Figure 6, which are much more easily visualized in the three-dimensional Southern Ocean schematic of Figure 4. The 6 Sv of SAMW/AAIW that move northward into the Indian and Pacific (subducting into the lower thermocline of the subtropical gyres) upwell diapycnally into the upper thermocline, joined by the 5 Sv upwelling from deeper down. These 11 Sv exit the Indian Ocean (physically in the Agulhas) and enter the South Atlantic, joined by the 2 Sv of Atlantic SAMW/AAIW, for a net northward flow of 13 Sv in the upper thermocline to feed into the NADW overturn. (However, the heat fluxes discussed next suggest that the Agulhas water does not directly flow into the South Atlantic. It is first cooled by a large amount, most

likely along the Agulhas Return Current, becoming SAMW/AAIW, and then enters the South Atlantic via the “cold water” route of Rintoul [1991].)

Lumpkin and Speer (2007) describe an additional pathway for the least dense NADW; they find approximately 7 Sv of NADW flowing southward out of the Atlantic at a neutral density lower than 27.6 γ^N . This water is light enough to join the IDW/PDW, upwell to the surface in the ACC, join the northward Ekman transport across the Subantarctic Front, and flow onward into the thermocline. This direct return path to the surface is the only part of the overturn that resembles the adiabatic theories of NADW overturn, but even in Lumpkin and Speer (2007), it represents only a fraction of the total NADW export from the Atlantic, with all of the denser NADW participating in the overturning circulation described herein—following a pathway through AABW formation, and then upwelling into the deepwater layers at low latitudes before returning to the Southern Ocean at a lower density. In our transport analysis (Talley et al., 2003; Talley, 2008), less than 2.5 Sv of low density NADW exit the South Atlantic, and so this part of the shallow overturning cell was not hypothesized or emphasized herein. This relative amount of warmed NADW transport is left as an open question for future transport analyses, but it is likely to be no larger than the Lumpkin and Speer (2007) value.

Heat Balance in the AABW and NADW Overturning Circulations

How much heating and cooling is associated with each of the transformations along the NADW and AABW circuits? We are especially interested in how much

heat is acquired subsurface through diapycnal diffusion compared with the amount that is exchanged through heating and cooling at the sea surface. Talley (2003) emphasized the much larger effects of heating/cooling when accomplished through air-sea fluxes versus the much weaker impact when accomplished through turbulent diffusion in the ocean interior. However, that is not to say that slower diffusive heating is unimportant—to the contrary, diffusion of heat downward into the abyssal waters is an essential part of the return of these waters to the surface. In the absence of such diffusion, the overturning circulation would be very different.

AABW formation in the Southern Ocean south of 32°S requires -0.35 PW heat loss from IDW/PDW and NADW, which upwell to the sea surface and are cooled (Figure 6b). North of 32°S, 0.26 PW heating of AABW and 0.09 PW heating of NADW create IDW/PDW, all through diapycnal diffusion of heat downward in the deep Indian and Pacific Oceans, closing the AABW heat balance.

Superimposed on formation of these waters is the global NADW cell. This cell is the more contorted loop in Figure 6, which looks somewhat like a figure eight. The NADW cell transports 0.29 PW northward across 32°S in the South Atlantic, of which 0.02 PW is due to flow of cold AABW northward into the Atlantic that upwells diffusively into NADW. Therefore, there must be a net heating of 0.27 PW outside the Atlantic that raises NADW back to upper ocean densities. Where does it happen?

This heat gain occurs in both the Southern Ocean south of 32°S and the Indian/Pacific north of 32°S. To the south, in the Southern Ocean, both near

and south of the ACC, where the IDW/PDW upwells to the sea surface, there is 0.13 PW of (surface) heating, sending 10 Sv northward to the subtropical thermocline (SAMW).

Where does the rest of the 0.14 PW warming occur? North of 32°S in the Indian and Pacific Ocean, there is 0.23 PW warming of IDW/PDW to join the lower thermocline and 0.6 PW warming of IDW/PDW to join the upper thermocline. The first of these warmings is likely diffusive; the latter could arguably be more strongly related to surface forcing and vigorous mixing that occurs especially in regions like the Indonesian passages through which the thermocline waters of the Pacific pass (e.g., Field and Gordon, 1992; Talley and Sprintall, 2005; Koch-Larrouy et al., 2008).

This 0.83 PW of warming in the Indian and Pacific is offset by -0.70 PW of cooling of upper thermocline waters exiting the Agulhas, south of 32°S, before they enter the South Atlantic, adding to 0.13 PW, which is within round-off error of the required 0.14 PW. It was long ago noted (Rintoul, 1991) that northward upper ocean flow in the South Atlantic is significantly cooler than the warm Agulhas southward flow. The large cooling of the surface waters occurs along the north side of the Agulhas Return Current (Large and Yeager, 2009; Cerovečki et al., 2011) and advects much of the Agulhas water southeastward toward Kerguelen. This cooled water joins the eastward flow of SAMW north of the ACC. The final product, SAMW/AAIW, flows northward in the South Atlantic, dominating the return to the Atlantic of upper ocean waters that feed into the NADW cell.

To summarize, the different blocks of

heating required for the NADW return flow can be divided in several ways.

The simplest message from the above is that about half (0.13 PW) of the heating occurs at the surface in the Southern Ocean and half (0.13 to 0.14 PW) is taken care of by interior diapycnal heating in the Indian and Pacific Oceans. A more complicated message is that the latter 0.14 PW includes 0.23 PW of intermediate-depth diapycnal diffusion, 0.6 PW of thermocline mixing that could have contributions from a range of mixing processes in addition to internal wave turbulence, and -0.7 PW of surface cooling.

So, while it has often been surmised that heating of the NADW cell can be accomplished south of 32°S within and north of the ACC (e.g., review in Marshall and Speer, 2012) through warming of the northward surface Ekman transport that moves upwelled ACC surface waters into the SAMW and thence into the subtropics, the NADW cell, as it exists, includes both full water-column diapycnal diffusion of heat in the mid- to low-latitude Indian and Pacific Oceans and surface heating in the Southern Ocean.

Diapycnal Upwelling and Deep Energy Balance Within the Atlantic Ocean

The NADW quantities and pathways described in the preceding paragraphs are focused on the circumpolar 32°S section. The overturning volume and heat transports are much higher across 24°N in the North Atlantic. This is not an artifact of the isopycnal layer choices. When the 24°N section is analyzed using the same isopycnal layers as the 32°S section, the southward NADW transport is

-25 Sv, northward AABW transport is 5 Sv, and northward transport above the NADW (above 36.8 σ_2) is 18 Sv. Thus, the transport of NADW is about 7 Sv higher at 24°N than at 32°S in this Reid (1994) velocity analysis. The NADW-associated northward heat transport across 24°N is 0.86 PW while it is only 0.26 PW across 32°S. Moreover, the NADW transport at 24°N is at a higher density than at 32°S. Thus, the NADW carried southward across 32°S has higher heat content and lower volume transport than at 24°N. The implied net heating is 0.6 PW between 24°N and 32°S through downward diapycnal diffusion into the NADW (Figure 6b). Lumpkin and Speer (2007) came to a very similar conclusion with their inverse model: they found a reduction in NADW transport from 18 Sv to 12 Sv between 24°N and 32°S and a shift to lower density at 32°S compared with 24°N, inferring net diapycnal heating in the NADW layer.

This result is vitally important: approximately half of the net Atlantic Ocean heating in the subtropics and tropics may percolate down to the NADW layer through diapycnal diffusion.

Inferred Diapycnal Diffusivities

The inferred downward diffusion of heat in the Atlantic is consistent with the rate of downward diffusion of heat in the Indian and Pacific Oceans. This suggests that the tropical and subtropical processes that create interior diapycnal diffusion are similar in all three oceans even though their deep waters behave so differently from one another, as previously inferred in Talley et al. (2003).

In Talley et al. (2003), a diapycnal diffusivity of $1-2 \times 10^{-4} \text{ m}^2 \text{ s}^{-1}$ was diagnosed for the low latitude abyssal

Atlantic, Indian, and Pacific Oceans based on the upwelling estimates summarized here, which were derived from basin-wide velocity analyses similar to those of inverse models. Macdonald et al. (2009), in an inverse model of Pacific Ocean circulation using all World Ocean Circulation Experiment (WOCE) hydrographic data, found average deep values that were a little less than $10^{-4} \text{ m}^2 \text{ s}^{-1}$, ranging up to about $1.5 \times 10^{-4} \text{ m}^2 \text{ s}^{-1}$ in the subtropical North Pacific. Lumpkin and Speer (2007), using an independent inverse model of ocean circulation, based on zonal WOCE hydrographic sections, inferred globally averaged diapycnal diffusivity between 32°S and 48°N (their Figure 5); they found heightened diffusivities of about $2 \times 10^{-4} \text{ m}^2 \text{ s}^{-1}$ in the bottommost layers, decreasing upward to about $1 \times 10^{-4} \text{ m}^2 \text{ s}^{-1}$ at the NADW level and decreasing further up into the thermocline.

These diffusivity estimates based on basin-scale transport estimates are remarkably similar to the Munk (1966) inferred value for the deep Pacific Ocean, which has held up with more modern budget studies (Munk and Wunsch, 1998; Wunsch and Ferrari, 2004). In contrast, Kunze et al. (2006), calculating diffusivity from a parameterization of internal wave shear and strain, found deep diffusivities of roughly half this size averaged over the ocean basins. In situ microstructure programs have found diffusivities that can be very low over large regions, but extremely elevated over rough topography (e.g., Armi, 1978; Polzin et al., 1997). Localized mixing hotspots could contribute disproportionately to thermocline to intermediate-depth mixing, such as found in the Indonesian Throughflow, where Pacific

waters that cross the sills between the sea surface and 1,940 m are mixed vigorously before exiting into the Indian Ocean (Field and Gordon, 1992; Talley and Sprintall, 2005; Koch-Larrouy et al., 2008; Gordon et al., 2010). Recent work of Amy Waterhouse, Scripps Institution of Oceanography, and colleagues syn-

part of the return of deep and bottom waters to the sea surface. Diapycnal heating of AABW at 0.2 to 0.3 PW in the Indian/Pacific Oceans closes one major part of the GOC, returning IDW/PDW to the Southern Ocean to be cooled and recycled into AABW. Additional diapycnal heating of the same rate is also essen-

“ THE GLOBAL OVERTURNING PATHWAYS FOR THE WELL-VENTILATED NORTH ATLANTIC DEEP WATER AND ANTARCTIC BOTTOM WATER AND THE DIFFUSIVELY FORMED INDIAN DEEP WATER AND PACIFIC DEEP WATER ARE INTERTWINED. ”

thesizes a large global set of deep microstructure observations as well as diffusivities inferred from parameterizations, and finds that there are sufficient regions of elevated diffusivity to result in large-scale averaged diffusivity of $10^{-4} \text{ m}^2 \text{ s}^{-1}$, thus supporting the results based on basin-scale velocity analyses.

DISCUSSION

The global overturning pathways for the well-ventilated North Atlantic Deep Water and Antarctic Bottom Water and the diffusively formed Indian Deep Water and Pacific Deep Water are intertwined. The global overturning circulation, and especially its heat balance, cannot be described without including *both* the volumetrically large wind-driven upwelling in the Southern Ocean and the similarly large internal diapycnal transformation in the deep Indian and Pacific Oceans.

Diapycnal heating in the deep tropical and subtropical ocean is a fundamental

tial for returning NADW to the sea surface, mostly through the circuitous route of first *cooling* to become AABW and then warming and upwelling in the deep Indian and Pacific Oceans. The contribution to the overall heating for the NADW loop from surface air-sea fluxes in the Southern Ocean is 0.13 PW, less than half the 0.29 PW that enters through diapycnal mixing at lower latitudes.

Many aspects of the global overturning circulation are not explored here, including the potential for an export from the South Atlantic of low density NADW directly to the upper overturning cell in the Southern Ocean, which emerges from Lumpkin and Speer's (2007) transport analysis and is featured in Marshall and Speer (2012). This light NADW export is much weaker in the transport analysis herein and likely reflects uncertainty due to differences in approaches to the initial velocity analysis and possibly differences in the results using two different sections (32°S herein vs. WOCE A11 in Lumpkin

and Speer, 2007). A second aspect is where and how NADW, IDW, and PDW upwell and mix in the Southern Ocean, and the intermediate contributions to AABW of the deep waters formed in the Antarctic that are both lighter and denser than the AABW layer that fills the oceans north of the ACC. Moreover, there is a large quasi-adiabatic exchange of Circumpolar Deep Waters and NADW, IDW, and PDW within their ocean basins. Separating them into net transports of CDW and NADW versus local eddy recirculations requires further water mass analysis along the lines of Johnson's (2008) global-scale analysis of the volume of deep and bottom water of Antarctic vs. North Atlantic origin.

DEDICATION

This is a contribution to the special volume of *Oceanography* dedicated to Peter Niiler. While Peter might have had issues with this kind of schematized global overturning circulation had he seen it, his long interest in ocean circulation and heat budgets, from idealized models to global-scale observations, were an inspiration to think on the largest scales.

ACKNOWLEDGMENTS

This work was supported by National Science Foundation grant OCE-0927650, with additional sabbatical support from Woods Hole Oceanographic Institution and LEGI/OSUG at the Université Joseph Fourier in Grenoble. This work was only possible because of J.L. Reid's meticulous global velocity analyses and generosity in sharing them. Conversations with J.L. Reid and J.P. Severinghaus are gratefully acknowledged, as are reviews from R. Lumpkin and A. Gordon. 

REFERENCES

- Armi, L. 1978. Some evidence for boundary mixing in the deep ocean. *Journal of Geophysical Research* 83:1,971–1,979, <http://dx.doi.org/10.1029/JC083iC04p01971>.
- Broecker, W.S. 1987. The biggest chill. *Natural History* 97:74–82.
- Broecker, W.S. 1991. The great ocean conveyor. *Oceanography* 4(2):79–89, <http://dx.doi.org/10.5670/oceanog.1991.07>.
- Cerovecki, I., L.D. Talley, and M.R. Mazloff. 2011. A comparison of Southern Ocean air-sea buoyancy flux from an ocean state estimate with five other products. *Journal of Climate* 24:6,283–6,306, <http://dx.doi.org/10.1175/2011JCLI3858.1>.
- Cerovecki, I., L.D. Talley, M.R. Mazloff, and G. Maze. In press. Subantarctic Mode Water formation, destruction and export in the eddy-permitting Southern Ocean State Estimate. *Journal of Physical Oceanography*.
- Ffield, A., and A.L. Gordon. 1992. Vertical mixing in the Indonesian thermocline. *Journal of Physical Oceanography* 22:184–195, [http://dx.doi.org/10.1175/1520-0485\(1992\)022<0184:VMITIT>2.0.CO;2](http://dx.doi.org/10.1175/1520-0485(1992)022<0184:VMITIT>2.0.CO;2).
- Ganachaud, A., and C. Wunsch. 2000. Improved estimates of global ocean circulation, heat transport and mixing from hydrographic data. *Nature* 408:453–456, <http://dx.doi.org/10.1038/35044048>.
- Ganachaud, A., and C. Wunsch. 2003. Large-scale ocean heat and freshwater transports during the World Ocean Circulation Experiment. *Journal of Climate* 16:696–705, [http://dx.doi.org/10.1175/1520-0442\(2003\)016<0696:LSOHAF>2.0.CO;2](http://dx.doi.org/10.1175/1520-0442(2003)016<0696:LSOHAF>2.0.CO;2).
- Gill, A.E., and K. Bryan. 1971. Effects of geometry on the circulation of a three-dimensional Southern-Hemisphere ocean model. *Deep Sea Research and Oceanographic Abstracts* 90:3,332–3,342, [http://dx.doi.org/10.1016/0011-7471\(71\)90086-6](http://dx.doi.org/10.1016/0011-7471(71)90086-6).
- Gnanadesikan, A. 1999. A simple predictive model for the structure of the oceanic pycnocline. *Science* 283:2,077–2,079, <http://dx.doi.org/10.1126/science.283.5410.2077>.
- Gordon, A.L. 1986a. Inter-ocean exchange of thermocline water. *Journal of Geophysical Research* 91:5,037–5,046, <http://dx.doi.org/10.1029/JC091iC04p05037>.
- Gordon, A.L. 1986b. Is there a global scale ocean circulation? *Eos, Transactions American Geophysical Union* 67(9):109–110, <http://dx.doi.org/10.1029/EO067i009p0109>.
- Gordon, A. 1991. The role of thermohaline circulation in global climate change. Pp. 44–51 in *Lamont-Doherty Geological Observatory 1990 & 1991 Report*. Lamont-Doherty Geological Observatory of Columbia University, Palisades, New York. Available at http://www.Ideo.columbia.edu/~agordon/publications/Gordon_Schematic_1991_LDEO_newsletter_.pdf (accessed February 18, 2013).
- Gordon, A.L., J. Sprintall, H.M. Van Aken, D. Susanto, S. Wijffels, R. Molcard, A. Ffield, W. Pranowo, and S. Wirasantosa. 2010. The Indonesian Throughflow during 2004–2006 as observed by the INSTANT program. *Dynamics of Atmosphere and Oceans* 50:115–128, <http://dx.doi.org/10.1016/j.dynatmoce.2009.12.002>.
- Jackett, D.R., and T.J. McDougall. 1997. A neutral density variable for the world's oceans. *Journal of Physical Oceanography* 27:237–263, [http://dx.doi.org/10.1175/1520-0485\(1997\)027<0237:ANDVFT>2.0.CO;2](http://dx.doi.org/10.1175/1520-0485(1997)027<0237:ANDVFT>2.0.CO;2).
- Johnson, G.C. 2008. Quantifying Antarctic Bottom Water and North Atlantic Deep Water volumes. *Journal of Geophysical Research* 113, C05027, <http://dx.doi.org/10.1029/2007JC004477>.
- Koch-Larrouy, A., G. Madec, D. Iudicone, A. Atmadipoera, and R. Molcard. 2008. Physical processes contributing to the water mass transformation of the Indonesian Throughflow. *Ocean Dynamics* 58:275–288, <http://dx.doi.org/10.1007/s10236-008-0154-5>.
- Koltermann, K.P., V.V. Gouretski, and K. Jancke. 2011. *Hydrographic Atlas of the World Ocean Circulation Experiment (WOCE): Volume 3. Atlantic Ocean*. M. Sparrow, P. Chapman, and J. Gould, eds, International WOCE Project Office, Southampton, UK. Available online at http://www-pord.ucsd.edu/whp_atlas/atlantic_index.html (accessed January 24, 2013).
- Kuhlbrodt, T., A. Griesel, M. Montoya, A. Levermann, M. Hofmann, and S. Rahmstorf. 2007. On the driving processes of the Atlantic meridional overturning circulation. *Reviews of Geophysics* 45, RG2001, <http://dx.doi.org/10.1029/2004RG000166>.
- Large, W.G., and S.G. Yeager. 2009. The global climatology of an interannually varying air-sea flux data set. *Climate Dynamics* 33:341–364, <http://dx.doi.org/10.1007/s00382-008-0441-3>.
- Lumpkin, R., and K. Speer. 2007. Global ocean meridional overturning. *Journal of Physical Oceanography* 37:2,550–2,562, <http://dx.doi.org/10.1175/JPO3130.1>.
- Macdonald, A.M., S. Mecking, J.M. Toole, P.E. Robbins, G.C. Johnson, S.E. Wijffels, L. Talley, and M. Cook. 2009. The WOCE-era 3-D Pacific Ocean circulation and heat budget. *Progress in Oceanography* 82:281–325, <http://dx.doi.org/10.1016/j.pocan.2009.08.002>.
- Maltrud, M.E., and J.L. McClean. 2005. An eddy resolving global 1/10° ocean simulation. *Ocean Modelling* 8:31–54, <http://dx.doi.org/10.1016/j.ocemod.2003.12.001>.
- Marshall, J., and T. Radko. 2003. Residual-mean solutions for the Antarctic circumpolar current and its associated overturning circulation. *Journal of Physical*

- Oceanography* 33:2,341–2,354, [http://dx.doi.org/10.1175/1520-0485\(2003\)033<2341:RSFTAC>2.0.CO;2](http://dx.doi.org/10.1175/1520-0485(2003)033<2341:RSFTAC>2.0.CO;2).
- Marshall, J., and K. Speer. 2012. Closure of the meridional overturning circulation through Southern Ocean upwelling. *Nature Geoscience* 5:171–180, <http://dx.doi.org/10.1038/ngeo1391>.
- Mazloff, M.R., P. Heimbach, and C. Wunsch. 2010. An eddy-permitting Southern Ocean state estimate. *Journal of Physical Oceanography* 40:880–899, <http://dx.doi.org/10.1175/2009JPO4236.1>.
- McDonagh, E.L., H.L. Bryden, B.A. King, and R.J. Sanders. 2008. The circulation of the Indian Ocean at 32°S. *Progress in Oceanography* 79:20–36, <http://dx.doi.org/10.1016/j.pocean.2008.07.001>.
- Merz, A., and G. Wüst. 1922. Die Atlantische Vertikalzirkulation. *Zeitschrift der Gesellschaft für Erdkunde zu Berlin* 1–35.
- Munk, W. 1966. Abyssal recipes. *Deep Sea Research and Oceanographic Abstracts* 13:707–730, [http://dx.doi.org/10.1016/0011-7471\(66\)90602-4](http://dx.doi.org/10.1016/0011-7471(66)90602-4).
- Munk, W., and C. Wunsch. 1998. Abyssal recipes II: Energetics of tidal and wind mixing. *Deep Sea Research Part I* 45:1,977–2,010, [http://dx.doi.org/10.1016/S0967-0637\(98\)00070-3](http://dx.doi.org/10.1016/S0967-0637(98)00070-3).
- Orsi, A.H., and T. Whitworth III. 2004. *Hydrographic Atlas of the World Ocean Circulation Experiment (WOCE): Volume 1. Southern Ocean*. M. Sparrow, P. Chapman, and J. Gould, eds, International WOCE Project Office, Southampton, UK. Available online at: <http://woceatlas.tamu.edu> (accessed January 24, 2013).
- Polzin, K.L., J. Toole, J.R. Ledwell, and R. Schmitt. 1997. Spatial variability of turbulent mixing in the abyssal ocean. *Science* 276:93–96, <http://dx.doi.org/10.1126/science.276.5309.93>.
- Rahmstorf, S. 2002. Ocean circulation and climate during the past 120,000 years. *Nature* 419:207–214, <http://dx.doi.org/10.1038/nature01090>.
- Reid, J.L. 1994. On the total geostrophic circulation of the North Atlantic Ocean: Flow patterns, tracers and transports. *Progress in Oceanography* 33:1–92, [http://dx.doi.org/10.1016/0079-6611\(94\)90014-0](http://dx.doi.org/10.1016/0079-6611(94)90014-0).
- Reid, J.L. 1997. On the total geostrophic circulation of the Pacific Ocean: Flow patterns, tracers and transports. *Progress in Oceanography* 39:263–352, [http://dx.doi.org/10.1016/S0079-6611\(97\)00012-8](http://dx.doi.org/10.1016/S0079-6611(97)00012-8).
- Reid, J.L. 2003. On the total geostrophic circulation of the Indian Ocean: Flow patterns, tracers and transports. *Progress in Oceanography* 56:137–186, [http://dx.doi.org/10.1016/S0079-6611\(02\)00141-6](http://dx.doi.org/10.1016/S0079-6611(02)00141-6).
- Richardson, P.L. 2008. On the history of meridional overturning circulation schematic diagrams. *Progress in Oceanography* 76:466–486, <http://dx.doi.org/10.1016/j.pocean.2008.01.005>.
- Rintoul, S.R. 1991. South Atlantic inter-basin exchange. *Journal of Geophysical Research* 96:2,675–2,692, <http://dx.doi.org/10.1029/90JC02422>.
- Robbins, P.E., and J.M. Toole. 1997. The dissolved silica budget as a constraint on the meridional overturning circulation in the Indian Ocean. *Deep Sea Research Part I* 44:879–906, [http://dx.doi.org/10.1016/S0967-0637\(96\)00126-4](http://dx.doi.org/10.1016/S0967-0637(96)00126-4).
- Sarmiento, J.L., N. Gruber, M.A. Brzezinski, and J.P. Dunne. 2004. High-latitude controls of thermocline nutrients and low latitude biological productivity. *Nature* 427:56–60, <http://dx.doi.org/10.1038/nature10605>.
- Schmitz, W.J. 1995. On the interbasin-scale thermohaline circulation. *Reviews of Geophysics* 33:151–173, <http://dx.doi.org/10.1029/95RG00879>.
- Schmitz, W.J. 1996. On the World Ocean Circulation: Volume I. Some global features/North Atlantic circulation. *Woods Hole Oceanographic Institution Technical Report*. WHOI-96-03, Woods Hole, MA, 141 pp.
- Sloyan, B.M., and S.R. Rintoul. 2001. The Southern Ocean limb of the global deep overturning circulation. *Journal of Physical Oceanography* 31:143–173, [http://dx.doi.org/10.1175/1520-0485\(2001\)031<0143:TSOLOT>2.0.CO;2](http://dx.doi.org/10.1175/1520-0485(2001)031<0143:TSOLOT>2.0.CO;2).
- Speer, K., S.R. Rintoul, and B. Sloyan. 2000. The diabatic Deacon cell. *Journal of Physical Oceanography* 30:3,212–3,222, [http://dx.doi.org/10.1175/1520-0485\(2000\)030<3212:TDDC>2.0.CO;2](http://dx.doi.org/10.1175/1520-0485(2000)030<3212:TDDC>2.0.CO;2).
- Speich, S., B. Blanke, P. de Vries, S. Drijfhout, K. Döös, A. Ganachaud, and R. Marsh. 2002. Tasman leakage: A new route in the global ocean conveyor belt. *Geophysical Research Letters* 29(10), <http://dx.doi.org/10.1029/2001GL014586>.
- Talley, L.D. 2003. Shallow, intermediate, and deep overturning components of the global heat budget. *Journal of Physical Oceanography* 33:530–560, [http://dx.doi.org/10.1175/1520-0485\(2003\)033<0530:SIADOC>2.0.CO;2](http://dx.doi.org/10.1175/1520-0485(2003)033<0530:SIADOC>2.0.CO;2).
- Talley, L.D. 2007. *Hydrographic Atlas of the World Ocean Circulation Experiment (WOCE): Volume 2. Pacific Ocean*. M. Sparrow, P. Chapman, and J. Gould, eds, International WOCE Project Office, Southampton, UK. Available online at: http://www-pord.ucsd.edu/whp_atlas/pacific_index.html (accessed January 24, 2013).
- Talley, L.D. 2008. Freshwater transport estimates and the global overturning circulation: Shallow, deep and throughflow components. *Progress in Oceanography* 78:257–303, <http://dx.doi.org/10.1016/j.pocean.2008.05.001>.
- Talley, L.D. 2011. *Hydrographic Atlas of the World Ocean Circulation Experiment (WOCE): Volume 4. Indian Ocean*. M. Sparrow, P. Chapman, and J. Gould, eds, International WOCE Project Office, Southampton, UK. Available online at: http://www-pord.ucsd.edu/whp_atlas/indian_index.html (accessed January 24, 2013).
- Talley, L.D., G.E. Pickard, W.J. Emery, and J.H. Swift. 2011. *Descriptive Physical Oceanography: An Introduction*, 6th ed. Elsevier, Burlington, MA, 560 pp.
- Talley, L.D., J.L. Reid, and P.E. Robbins. 2003. Data-based meridional overturning stream-functions for the global ocean. *Journal of Climate* 16:3,213–3,226, [http://dx.doi.org/10.1175/1520-0442\(2003\)016<3213:DMOSFT>2.0.CO;2](http://dx.doi.org/10.1175/1520-0442(2003)016<3213:DMOSFT>2.0.CO;2).
- Talley, L.D., and J. Sprintall. 2005. Deep expression of the Indonesian Throughflow: Indonesian Intermediate Water in the South Equatorial Current. *Journal of Geophysical Research* 110, C10009, <http://dx.doi.org/10.1029/2004JC002826>.
- Toggweiler, J.R., and B. Samuels. 1995. Effect of Drake Passage on the global thermohaline circulation. *Deep-Sea Research Part I* 42:477–500, [http://dx.doi.org/10.1016/0967-0637\(95\)00012-U](http://dx.doi.org/10.1016/0967-0637(95)00012-U).
- Toole, J.M., and B.A. Warren. 1993. A hydrographic section across the subtropical South Indian Ocean. *Deep-Sea Research Part I* 40:1,973–2,019, [http://dx.doi.org/10.1016/0967-0637\(93\)90042-2](http://dx.doi.org/10.1016/0967-0637(93)90042-2).
- Warren, B.A. 1990. Suppression of deep oxygen concentrations by Drake Passage. *Deep Sea Research Part A* 37:1,899–1,907, [http://dx.doi.org/10.1016/0198-0149\(90\)90085-A](http://dx.doi.org/10.1016/0198-0149(90)90085-A).
- Wolfe, C.L., and P. Cessi. 2011. The adiabatic pole-to-pole overturning circulation. *Journal of Physical Oceanography* 41:1,795–1,810, <http://dx.doi.org/10.1175/2011JPO4570.1>.
- Wunsch, C., and R. Ferrari. 2004. Vertical mixing, energy and the general circulation of the oceans. *Annual Review of Fluid Mechanics* 36:281–314, <http://dx.doi.org/10.1146/annurev.fluid.36.050802.122121>.